

# Slip Sliding Away: Load-Dependence of Velocity Generated by Skeletal Muscle Myosin Molecules in the Laser Trap

Edward P. Debold, Joseph B. Patlak, and David M. Warshaw

Department of Molecular Physiology & Biophysics, University of Vermont, Burlington, Vermont 05405

**ABSTRACT** Skeletal muscle's ability to shorten and lengthen against a load is a fundamental property, presumably reflecting the inherent load-dependence of the myosin molecular motor. Here we report the velocity of a single actin filament translocated by a mini-ensemble of skeletal myosin  $\sim 8$  heads under constant loads up to 15 pN in a laser trap assay. Actin filament velocity decreased with increasing load hyperbolically, with unloaded velocity and stall force differing by a factor of 2 with [ATP] (30 vs. 100  $\mu\text{M}$ ). Analysis of actin filament movement revealed that forward motion was punctuated with rapid backward 60-nm slips, with the slip frequency increasing with resistive load. At stall force, myosin-generated forward movement was balanced by backward slips, whereas at loads greater than stall, myosin could no longer sustain forward motion, resulting in negative velocities as in eccentric contractions of whole muscle. Thus, the force-velocity relationship of muscle reflects both the inherent load-dependence of the actomyosin interaction and the balance between forward and reverse motion observed at the molecular level.

Received for publication 19 August 2005 and in final form 29 August 2005.

Address reprint requests and inquiries to David Warshaw, Tel.: 802-656-4300; Fax: 802-656-0747;

E-mail: warshaw@physiology.med.uvm.edu.

Muscle's ability to generate force and motion is due to numerous myosin molecular motors interacting cyclically with actin, a process powered by myosin's hydrolysis of ATP. The velocity at which a skeletal muscle shortens is load-dependent, slowing with increasing load as described by the now classic hyperbolic force-velocity (F:V) relationship (1). At loads greater than a muscle's maximum isometric force, the muscle is forced to lengthen (i.e., eccentric contraction), even though myosin molecules interact with actin to resist this motion. Fifty years ago, A. F. Huxley proposed that load can affect one or more steps in myosin's cyclic interaction with actin (2), which he based largely on the shape of the F:V relationship from whole muscle. Given the complexities inherent to muscle tissue, the ability to relate muscle mechanical properties to the underlying kinetics and mechanics of the myosin motor is far from certain. Therefore, we characterized the F:V relationship at the molecular level in a laser trap by measuring the velocity of a single actin filament being displaced by a mini-ensemble (approximately eight heads) of skeletal muscle myosin motors under constant load. Such measurements would be impossible with a single skeletal myosin molecule due to its low unloaded duty ratio (i.e.,  $\sim 4\%$ ) (3), thus necessitating the use of a mini-ensemble and subsaturating ATP.

Using a software-controlled, force clamp (4) in a three-bead laser trap assay (5), we applied 1–15 pN constant loads to a rigid bead-actin-bead assembly. On contact with the myosin-coated surface, the bead-actin-bead assembly would begin to slide. Constant load was then applied by keeping the position of the trap center relative to the bead constant (i.e., force clamped) using an acousto-optic deflector. A series of sequential load steps, with each step lasting 80–200 ms, was

applied repeatedly in increasing and then decreasing order (Fig. 1 B). Comparison of velocities at a given load, whether obtained during the rising or falling load sequence, had no effect on the resultant velocity (data not shown).

Actin filament velocity at each load was determined as the slope of the linear regression through the displacement record (Fig. 1 C). Multiple velocity measurements for each load were then averaged for a given experiment (i.e., a given actin filament) and then averaged across multiple actin filaments to generate a F/V relationship (Fig. 1 A). Purified whole chicken pectoralis skeletal myosin was adhered (15  $\mu\text{g}/\text{ml}$ ) to a nitrocellulose-coated silica bead pedestal. Knowing the myosin density (3), a minimum of eight myosin heads could interact with the 0.5  $\mu\text{m}$  of actin filament that was presented to the surface. The final assay buffer was 25 mM KCl-actin buffer with either 30 or 100  $\mu\text{M}$  ATP at 20°C (5).

Actin filament velocity decreased with increasing load from its unloaded maximum until loads sufficient to stall the actin filament were reached (Fig. 1 A). At loads greater than the stall force, the myosin could no longer support continuous forward motion, resulting in the actin filament being effectively pulled backward by the laser trap. Interestingly, loads applied in the direction of actin filament motion (30  $\mu\text{M}$  ATP only) resulted in velocities  $3\times$  faster than unloaded values, which were limited by the filament's interaction with myosin and not the capacity of the instrumentation. The observed F:V relationships obtained at both 30 and 100  $\mu\text{M}$  ATP (Fig. 1 A) were well fit ( $p < 0.02$ ) by Hill's hyperbolic F:V equation (1), i.e.,  $(F + a)(V +$

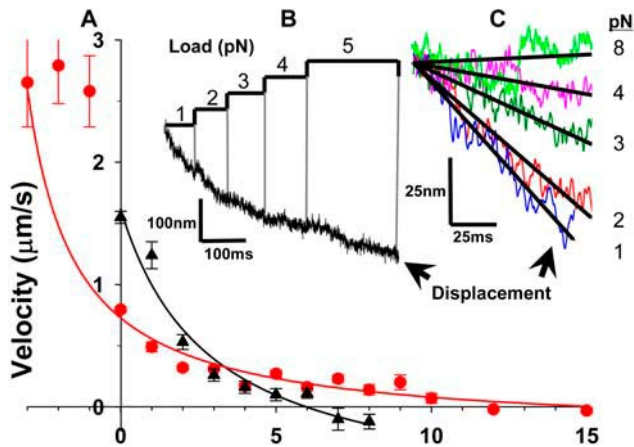


**FIGURE 1** (A) F/V data at 30  $\mu\text{M}$  (red circles) and 100  $\mu\text{M}$  ATP (black triangles) as means  $\pm$  SE. Hill F/V fit to positive loads only (lines; see text) at 30  $\mu\text{M}$  ATP ( $F_0 = 15$  pN,  $a/F_0 = 0.29$ ,  $b = 0.21$   $\mu\text{m/s}$ ) and 100  $\mu\text{M}$  ATP ( $F_0 = 6$  pN,  $a/F_0 = 0.33$ ,  $b = 0.53$   $\mu\text{m/s}$ ). (B) Only increasing load sequence shown with force levels above displacement trace. (C) Filtered actin displacement traces (at 100  $\mu\text{M}$  ATP) at different loads with their respective linear regressions used to determine actin filament velocity; 10–90 velocities at each load were averaged to generate F/V in panel A.

$b) = (F_0 + a)b$ , where  $F_0$  is the stall force and  $a$  and  $b$  are constants of the fit. There was no a priori reason to assume this relationship, but the curvature, indicated by the  $a/F_0$  values (0.29 and 0.33 for 30 and 100  $\mu\text{M}$  ATP, respectively) was strikingly similar to that reported for whole skeletal muscle (0.11–0.48) (6). Furthermore, the shift in the F/V relationship going from 100 to 30  $\mu\text{M}$  ATP, where both the unloaded maximum velocity decreases and the stall force increases by a factor of 2, is consistent with that seen in muscle fibers with reduced ATP (7).

With a relatively small number of myosin heads contributing to the observed actin filament velocities, the dynamics of filament motion under load are revealed. For resistive loads, an apparent dynamic instability exists where forward motion of the actin filament is interrupted by occasional, rapid ( $\tau \sim 2$  ms) backward slips (Fig. 2, A, inset). The slips have load-independent amplitudes of  $\sim 60$  nm (Fig. 2, B), whereas their frequency increases with load (Fig. 2, C). Because slips are greater than the 10-nm myosin step size (5), they are likely not simple reversals of a single power-stroke. Alternately, with such a limited number of heads, stochastic variation in the number of attached heads may lead to brief periods when only a few heads hold the entire load. The progressively higher load per head may induce subsequent detachment in the remaining heads, consistent with the slip frequency increasing with load. Once the last head detaches, the laser trap would then pull the actin filament backward at a rate limited by the system's response time (i.e.,  $\tau \sim 2$  ms, independent of load). Although capable

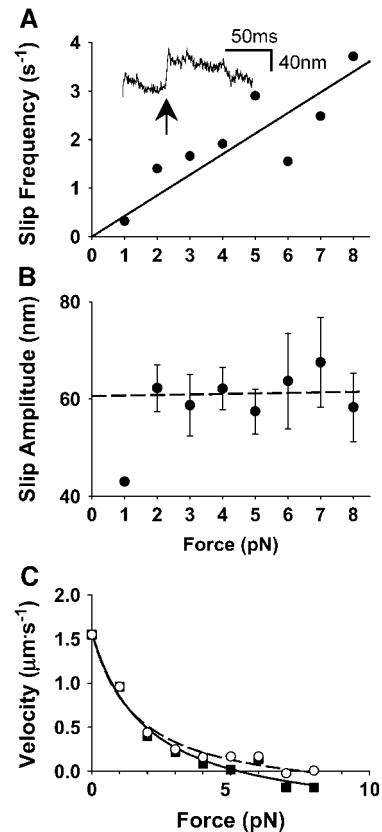


**FIGURE 2** Characterization of slips at 100  $\mu\text{M}$  ATP (similar results obtained at 30  $\mu\text{M}$  ATP). (A) Slip frequency versus load ( $r = 0.84$ ). Inset is a displacement record with a rapid reversal or "slip" in response to 5 pN. (B) Slip amplitude versus force, each point is the mean  $\pm$  SE. Regression omits 1-pN data yielding 60-nm average amplitude. (C) F/V data with (■, solid line) and without slips (○, dashed line) and fit with Hill F/V equation.

of moving  $>500$  nm, the distance traveled by the actin filament during a slip was limited to 60 nm on average (Fig. 2, B), suggesting that the slip distance is determined by the rate of head reattachment, which should be independent of load as was observed (Fig. 2, B). Finally, in the absence of ATP where myosin is tightly bound to actin in rigor, slips were not observed (data not shown), confirming that slips only occur when load is applied to an actin filament interacting with actively cycling myosin.

The F/V relationships described above (Fig. 1, A) were generated from displacement records whether or not a slip occurred. When the F/V relationship at 100  $\mu\text{M}$  ATP was reanalyzed by eliminating slips from the velocity determinations, it is not surprising that the backward slips contribute most to the shape of the F/V relationship near stall (Fig. 2, C), where the frequency of slips is highest. The slips have the net effect of reducing the estimated stall force by  $\sim 40\%$ . Thus, at stall force, where velocity is zero, forward motion generated by the myosin ensemble is balanced by backward slips, a concept similar to that reported for kinesin (8). At

forces greater than stall, the frequency of slips becomes sufficiently high to result in negative velocities, which may provide a molecular explanation for the lengthening response observed during eccentric contractions in whole muscle. Our ability to measure directly the frequency of slips, and the F/V behavior between them, should give new insight into the load dependence of the attached states of myosin, whereas studies of slip amplitude and duration should give insight into the attachment process itself.

At low resistive loads where slips are not as frequent and do not contribute significantly to the load-dependence of velocity, load may affect velocity by modulating the myosin step size (9) and/or the kinetics of specific steps in the actomyosin cycle (10). The extreme increase in velocity with assistive loads suggests that the myosin detachment rate is accelerated to a maximum value that is constant over the range of loads studied.

In addition to the externally applied load, internal loads created by neighboring myosin molecules within the ensemble that are simultaneously attached to the actin filament are an equally important consideration. With the ability to differentially label individual heads with fluorescent probes (11) it may be possible using single-molecule techniques to characterize how myosins within an ensemble communicate and interact to generate motion under load.

The F/V relationships obtained here for the miniensemble are an initial step in bridging the functional gap between the observations from a single myosin molecule and from the large ensemble of motors that exist in a muscle fiber. Although F/V relationships have been obtained previously using skeletal myosin filament-coated beads gliding over Nitella actin bundles (12), the straightforward geometry of this study and the limited number of myosin molecules eliminates much of the complexity associated with these earlier studies. Once characterized, the F/V relationship allows one to calculate myosin's power-generating capacity (i.e.,  $F \times V$ ) as a function of load, permitting characterization of normal and mutant myosins associated with cardiomyopathies over their full range of physiologic demand.

## ACKNOWLEDGMENTS

We thank A. Armstrong and S. Beck for their unending technical assistance, G. Kennedy for opto-mechanical support, and N. Kad and J. Baker for discussions throughout the project initiated by J. Moore.

This work was supported by the National Institutes of Health (AR47906, HL59408).

## REFERENCES and FOOTNOTES

1. Hill, A. V. 1938. The heat of shortening and the dynamic constants of muscle. *Proc. R. Soc. Lond. B. Biol. Sci.* 126:136–195.
2. Huxley, A. F. 1957. Muscle structure and theories of contraction. *Prog. Biophys. Biophys. Chem.* 7:255–318.
3. Harris, D. E., and D. M. Warshaw. 1993. Smooth and skeletal muscle myosin both exhibit low duty cycles *in vitro*. *J. Biol. Chem.* 268:14764–14768.
4. Visscher, K., M. J. Schnitzer, and S. M. Block. 1999. Single kinesin molecules studied with a molecular force clamp. *Nature*. 400:184–189.
5. Kad, N. M., A. S. Rovner, P. M. Fagnant, P. B. Joel, G. G. Kennedy, J. B. Patlak, D. M. Warshaw, and K. M. Trybus. 2003. A mutant heterodimeric myosin with one inactive head generates maximal displacement. *J. Cell Biol.* 162:481–488.
6. Woledge, R. C., N. A. Curtin, and E. Homsher. 1985 *Energetic Aspects of Muscle Contraction*. Academic Press, Orlando, FL.
7. Cooke, R., and W. Bialek. 1979. Contraction of glycerinated fibers as a function of ATP concentration. *Biophys. J.* 28:241–258.
8. Carter, N. J., and R. A. Cross. 2005. Mechanics of the kinesin step. *Nature*. 435:308–312.
9. Reconditi, M., M. Linari, L. Lucii, A. Stewart, Y. B. Sun, P. Boesecake, T. Narayanan, R. F. Fischetti, T. Irving, G. Piazzesi, G. Irving, and V. Lombardi. 2004. The myosin motor in muscle generates a smaller and slower working stroke at higher load. *Nature*. 428:578–581.
10. Veigel, C., J. E. Molloy, S. Schmitz, and J. Kendrick-Jones. 2003. Load-dependent kinetics of force production by smooth muscle myosin measured with optical tweezers. *Nat. Cell Biol.* 5:980–986.
11. Warshaw, D. M., G. G. Kennedy, S. S. Work, E. B. Kremntsova, S. Beck, and K. M. Trybus. 2005. Differential labeling of myosin V heads with quantum dots allows direct visualization of hand-over-hand processivity. *Biophys. J.* 88:L30–L32.
12. Oiwa, K., S. Chaen, E. Kamitsubo, T. Shimmen, and H. Sugi. 1990. Steady-state force velocity relation in the ATP-dependent sliding movement of myosin-coated beads on actin cables *in-vitro* studied with a centrifuge microscope. *Proc. Natl. Acad. Sci. USA.* 87:7893–7897.